Determining the magnetic permeability of ferrite steel strip by a custom inversion method

M. Lu[1], W. Zhu[1], W. Yin[1], F.D. van den Berg[2], H. Yang[2] and A. J. Peyton[1]

1 University of Manchester, United Kingdom, a.peyton@manchester.ac.uk
2 Tata Steel, The Netherlands, frenk.van-den-berg@tatasteel.com

Abstract

In this paper, an inverse method was developed which can, in principle, reconstruct arbitrary permeability, conductivity, thickness, and lift-off with a multi-frequency electromagnetic method from inductance spectroscopic measurements.
Both the finite element method and the Dodd and Deeds formulation are used to solve the forward problem during the inversion process. For the inverse solution, a modified Newton–Raphson method is used to adjust each set of parameters (permeability, conductivity, thickness, and lift-off) to fit inductances (measured or simulated) in a least-squared sense because of its known convergence properties. The approximate Jacobian matrix (sensitivity matrix) for each set of the parameter is obtained by the perturbation method. Results from an industrial-scale sensor are presented. The results are verified with measurements and simulations of selected cases.
The findings are significant because they show for the first time that the inductance spectra can be inverted in practice to determine the key values (permeability, conductivity, thickness, and lift-off) with a relative error of less than 5% during the thermal processing of metallic plates.

1. Introduction

Multi-frequency electromagnetic sensors, such as EMspec [1], are now being used to non-destructively test the properties of strip steel on-line during industrial processing. These sensors measure the relative permeability of the strip during process operations such as controlled cooling and the permeability values are analysed in real time to determine important microstructural parameters such as the transformed fraction of the required steel phases. These parameters are critical to achieving the desired mechanical properties in the strip product. The inductance spectra produced by the sensor are not only dependent on the magnetic permeability of the strip, but is also an unwanted function of the electrical conductivity and thickness of the strip and the distance between the strip steel and the sensor (lift-off). The confounding cross-sensitivities to these other parameters must be rejected by the processing algorithms applied to inductance spectra.

In recent years, the eddy current technique (ECT) [2-7] and the alternating current potential drop (ACPD) technique [8-10] are the two primary electromagnetic non-destructive testing techniques on metals' permeability measurements. However, the measurement of permeability is still a challenge due to the influence of conductivity, lift-off, and thickness on the detected signal. Therefore, decoupling the impact of the other parameters than permeability is quite vital in permeability measurement [11-13].

This paper considers the cross-sensitivity of the complex spectra from a multi-frequency inductance spectra to the four variables namely, permeability, conductivity, thickness, and lift-off with tested sensors. The paper then goes further to consider the solution of the inverse problem of determining unique values for the four variables from the spectra. There are two major computational problems in the reconstruction process: the forward problem and the inverse problem. The forward problem is to calculate the frequency-dependent inductance for metallic plates with arbitrary values of permeability, conductivity, thickness, and lift-off (i.e. the distance between the sensor and test sample). The inverse problem is to determine each profile's sensitivity, i.e. the changes in each profile (permeability, conductivity, thickness, and lift-off with tested sensors) from the changes in frequency-dependent inductance measurements. A dynamic rank method was proposed to eliminate the ill-conditioning of the problem in the process of reconstruction. Profiles of permeability, conductivity, thickness, and lift-off have been reconstructed from simulated and measured data using an EM sensor, which has verified this method.

2. Coil arrangement and sample information

The sensor is composed of three coaxially arranged coils, configured as an axial gradiometer; with the three coils having the same diameter, i.e. 150 mm. Each of the coils has 15 turns, and the coil separation is 35 mm. A photograph of the sensor is shown in Fig. 1. with its dimensions in Table 1. The central coil is a transmitter and the two outer coils are receivers and connected in series opposition. A Solartron Impedance Analyzer SI1260 is used to record the experimental sensor output data., The geometry of the sensor has also been designed so that a high temperature version can be fabricated for use at high temperatures in a production furnace and consequently magnetic components such as a magnetic yoke cannot be used. The detailed design of the

industrial high temperature version of the sensor is beyond the scope of this paper. The design of this sensor is such that both the finite-element method and the Dodd and Deeds formulation can be used to solve the forward problem during the inversion process.

The samples were chosen to be a series of dual-phase steel (DP steel) samples - DP600 steel (with an electrical conductivity of 4.13 MS/m, relative permeability of 222, and thickness of 1.40 mm) , DP800 steel (with an electrical conductivity of 3.81 MS/m, relative permeability of 144, and thickness of 1.70 mm), and DP1000 steel (with an electrical conductivity of 3.80 MS/m, relative permeability of 122, and thickness of 1.23 mm) and same planar dimensions of 500 × 400 mm size. The same probe was used for measurements at several lift-offs of 5 mm, 30 mm, 50 mm, and 100 mm.
.

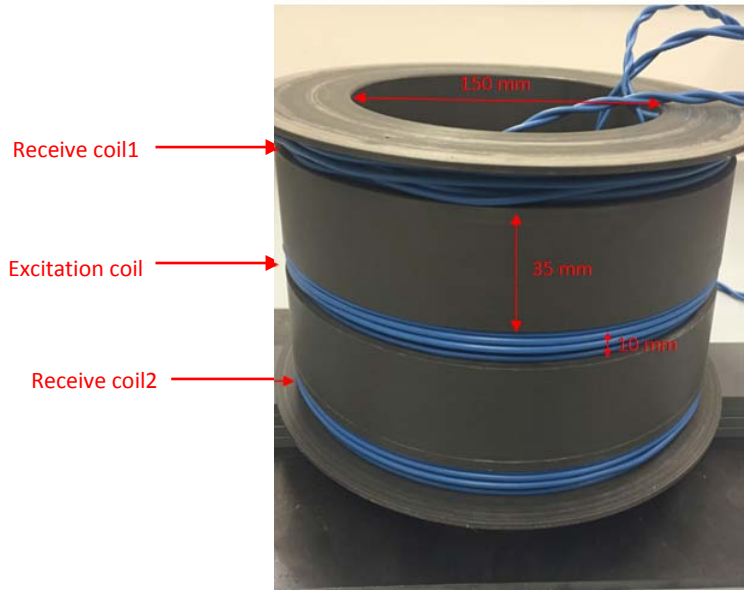

Figure 1. Sensor configuration

Table 1. Coil parameters

Inner diameter	150 mm
Outer diameter	175 mm
lift-offs	5, 30, 50, 100 mm
Coils height	10 mm
Coils gap	35 mm
Number of turns N1(coil1) = N2(coil2) = N3(coil3)	15

3. Proposed inverse solver

The inverse problem in this case is to determine the permeability, conductivity, thickness, and lift-off with tested sensors profiles from the frequency-dependent inductance measurements. A modified Newton–Raphson method [15]is used to adjust

each profile to fit inductances (measured or simulated) in a least-squared sense because of its known convergence properties.

Definition of the problem:

1) $L_0 \in R^m$: observed inductances arranged in a vector form (In this paper, a corresponded expansion matrix $\mathbf{L_0}$ with the real part and imaginary part of observed inductance listed on the top and bottom m rows of the matrix - i.e. $\mathbf{L_0} = [\mathrm{Re}(L_0); \mathrm{Im}(L_0)]$ is presented). And m is the number of frequencies at which the inductance measurements are taken (here we select 10 frequency samples, i.e. $m = 10$).

2) $\sigma \in R$: electrical conductivity of the tested sample.

3) $\mu \in R$: permeability of the tested sample.

4) $t \in R$: thickness of the tested sample.

5) $l \in R$: lift-off of the sensors with respect to the sample plate.

6) $f : R^n \to R^m$ is a function mapping an input signal **[σ μ t l]** with n degrees of freedom (here $n = 4$) into a set of m approximate inductance observations (In this paper, a corresponded expansion matrix $\mathbf{f}$ with real part and imaginary part of observed inductance listed on the top and bottom m rows of the matrix - i.e. $\mathbf{f} = [\mathrm{Re}(f);\mathrm{Im}(f)]$ is included). Here f can be calculated by the forward problem method such as Dodd and Deeds method.

7) $\phi = (1/2)[\mathbf{f} - \mathbf{L_0}]^{\mathbf{T}}[\mathbf{f} - \mathbf{L_0}]$ is the squared error of the measured and estimated inductance

Note that f is a function of sample's properties $(\boldsymbol{\sigma}, \boldsymbol{\mu}, \mathbf{t}, \mathbf{l})$ under fixed measurement arrangements. The problem is to find a point $(\boldsymbol{\sigma}^*, \boldsymbol{\mu}^*, \mathbf{t}^*, \mathbf{l}^*)$ that is at least a local minimum of the cost function ϕ.

The proposed inverse solver is shown as follows:

$$[\Delta\boldsymbol{\sigma}\ \Delta\boldsymbol{\mu}\ \Delta\mathbf{t}\ \Delta\mathbf{l}]^{\mathbf{T}} = -\left[\mathbf{J}^{\mathrm{T}}\mathbf{J}\right]^{-1}\mathbf{J}^{\mathrm{T}}\left[\mathbf{f}(\boldsymbol{\sigma}_{\mathbf{r}}, \boldsymbol{\mu}_{\mathbf{r}}, \mathbf{t}_{\mathbf{r}}, \mathbf{l}_{\mathbf{r}}) - \mathbf{L}_0\right] \quad (1)$$

$$[\boldsymbol{\sigma}\ \boldsymbol{\mu}\ \mathbf{t}\ \mathbf{l}]^{\mathbf{T}} = [\boldsymbol{\sigma}_{\mathbf{r}}\ \boldsymbol{\mu}_{\mathbf{r}}\ \mathbf{t}_{\mathbf{r}}\ \mathbf{l}_{\mathbf{r}}]^{\mathbf{T}} + [\Delta\boldsymbol{\sigma}\ \Delta\boldsymbol{\mu}\ \Delta\mathbf{t}\ \Delta\mathbf{l}]^{\mathbf{T}} \quad (2)$$

Where, **J** represents $\mathbf{f}(\boldsymbol{\sigma}, \boldsymbol{\mu}, \mathbf{t}, \mathbf{l}, \mathbf{r})$.

Equations (1) and (2) can be used in an iterative fashion to find $(\boldsymbol{\sigma}^*, \boldsymbol{\mu}^*, \mathbf{t}^*, \mathbf{l}^*)$. This formulation is known as the Gauss–Newton method. For each step in the iterative procedure, the Jacobian matrix **J** needs to be updated, which involves a considerable amount of computation.

Previously, Tikhonov regularization method has been widely used in many inverse problems to deal with the ill-conditioning in **J**. However, the estimated error resulting from the regularization cannot be neglected due to the amendment of the sensitivity matrix. Here, a dynamic rank method is adopted to maintain that the results are estimated from the original unmodified sensitivity matrix, which has much improved the estimation accuracy. The principle of the dynamic rank method is indexing the columns whose elements are all zeros. Then reduce the rank of the sensitivity matrix **J** by omitting the indexed columns. For each step in the iterative procedure, the corresponded rows of the estimated $[\Delta\boldsymbol{\sigma}\ \Delta\boldsymbol{\mu}\ \Delta\mathbf{t}\ \Delta\mathbf{l}]^{\mathbf{T}}$ should be valued zeros.

4. Parameter sensitivity of multi-frequency

Figure 2-5 illustrate the effects of different delta profiles $(\Delta\sigma\ \Delta\mu\ \Delta t\ \Delta l)$ on both the real part (a) and imaginary part (b) of the sensors and sample mutual inductance change rate on the referred point $(\sigma_r\ \mu_r\ t_r\ l_r)$ relative to samples' electrical conductivity ($\frac{Re(\Delta L)}{\Delta\sigma}$ and $\frac{Im(\Delta L)}{\Delta\sigma}$), relative permeability ($\frac{Re(\Delta L)}{\Delta\mu}$ and $\frac{Im(\Delta L)}{\Delta\mu}$), thickness ($\frac{Re(\Delta L)}{\Delta t}$ and $\frac{Im(\Delta L)}{\Delta t}$) and lift-off ($\frac{Re(\Delta L)}{\Delta l}$ and $\frac{Im(\Delta L)}{\Delta l}$). Here the referred point $(\sigma_r\ \mu_r\ t_r\ l_r)$ is selected to be the properties of DP 600 steel sample with property profiles of (4.13 MS/m 222 1.4 mm 5 mm).

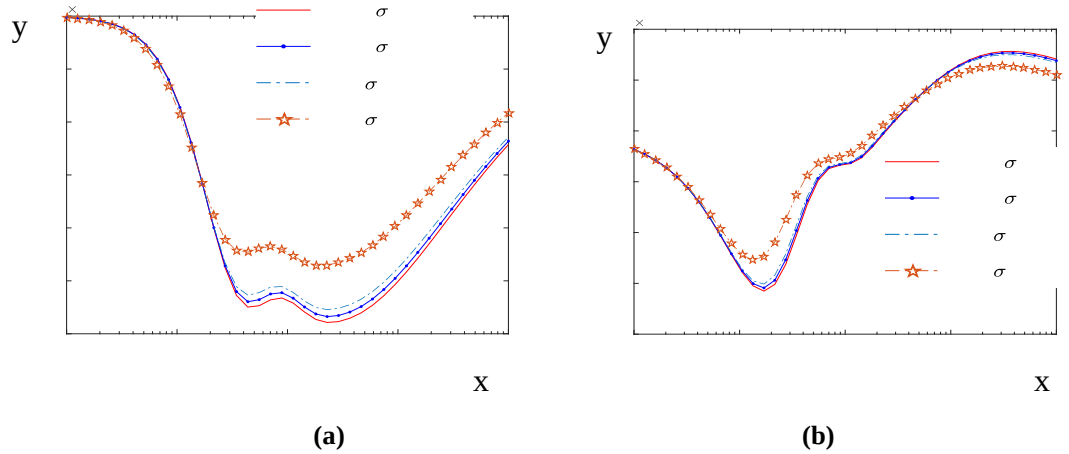

(a) **(b)**

Figure 2. Effects of different $(\Delta\sigma\ \Delta\mu\ \Delta t\ \Delta l)$ on both real part (a) and imaginary part (b) of conductivity sensitivity of the referred point (Re(ΔL)/Δσ and Im(ΔL)/Δσ)

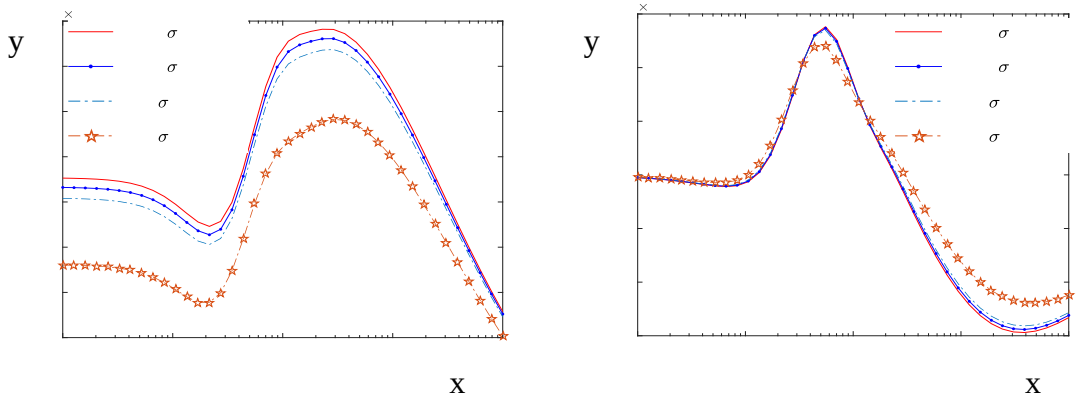

(a) **(b)**

Figure 3. Effects of different $(\Delta\sigma\ \Delta\mu\ \Delta t\ \Delta l)$ on both real part (a) and imaginary part (b) of relative permeability sensitivity of the referred point (Re(ΔL)/Δμ and Im(ΔL)/Δμ)

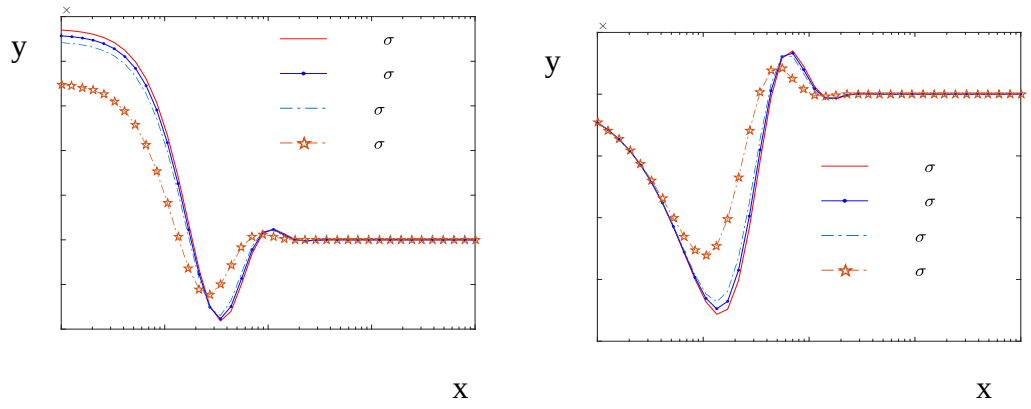

(a) **(b)**

Figure 4. Effects of different $(\Delta\sigma\ \Delta\mu\ \Delta t\ \Delta l)$ on both real part (a) and imaginary part (b) of sample thickness sensitivity of the referred point (Re(ΔL)/Δt and Im(ΔL)/Δt)

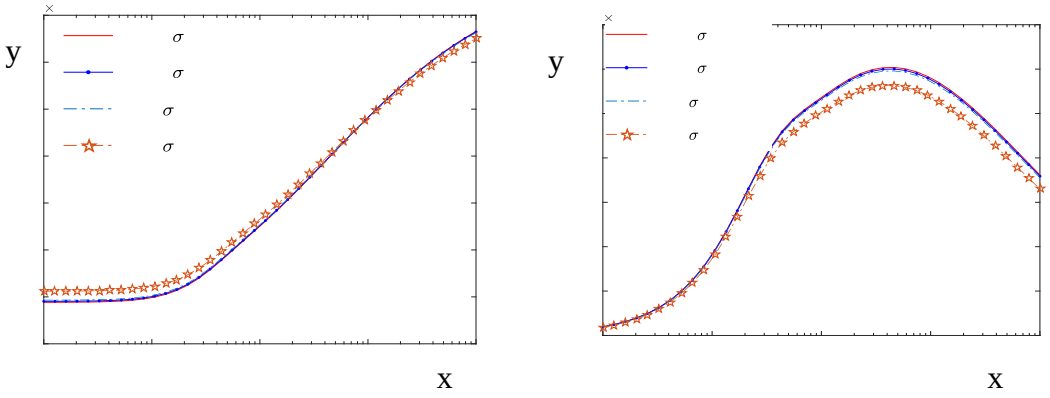

(a) **(b)**

Figure 5. Effects of different $(\Delta\sigma\ \Delta\mu\ \Delta t\ \Delta l)$ on both real part (a) and imaginary part (b) of sensors lift-offs sensitivity of the referred point (Re(ΔL)/Δl and Im(ΔL)/Δl)

Figures 2 to 5 show the frequency-dependent sensitivity of the sample electrical conductivity, relative permeability, sample thickness, and sensor lift-off when different delta profiles $[\Delta\sigma\ \Delta\mu\ \Delta t\ \Delta l]^T$ within in the sensitivity matrix is selected to be 1%, 5%, 10% and 50% of referred properties $[\sigma_r\ \mu_r\ t_r\ l_r]^T$ ([4.13 MS/m 222 1.4 mm 5 mm]) respectively. It is found that as we decrease the changes of $(\Delta\sigma\ \Delta\mu\ \Delta t\ \Delta l)$, the sensitivity curves approach a set of saturation curves. Further decreasing $(\Delta\sigma\ \Delta\mu\ \Delta t\ \Delta l)$ would not make a significant effect on sensitivity spectra.

5. Reconstruction

As can be seen from Table 2, the samples profiles are reconstructed accurately from both the measured inductance $\mathbf{L}_0$ and simulated data (parameters multi-frequency spectra **J** and simulated inductance **f**) with a relative error of less than 5%, which is achieved by utilizing the proposed dynamic rank method to eliminate the ill-conditioning problem in the process of reconstruction. (Here, the initial values $[\sigma_r\ \mu_r\ t_r\ l_r]^T$ for the iterative search of the solution are 5 M S/m, 100, 2 mm, and 4mm.) The proposed dynamic rank method is shown to be more efficient than the typical regularization method - Tikhonov regularization method [15].

Table 2. Reconstruction of the selected samples' properties (electrical conductivity relative permeability μ, sample thickness t, sensors lift-offs l) when calculated by the proposed inverse solver

	Actual value					Estimated value by the proposed inverse solver				
Case No.	1	2	3	4	5	1	2	3	4	5
Conductivity - σ (M S/m)	4.13	3.81	3.80	3.80	3.80	4.06	3.70	3.68	3.65	3.63
Relative permeability - μ	222	144	122	122	122	229	138	120	119	116
Thickness - t (mm)	1.40	1.70	1.23	1.23	1.23	1.41	1.69	1.23	1.23	1.24
Lift-off - l (mm)	5	5	5	30	50	5.02	5.03	5.06	30.41	50.63
Iteration No.	-	-	-			7	5	4	15	22

6. Conclusions

In this paper, a method is presented which has the potential to reconstruct an arbitrary permeability, conductivity, thickness, and lift-off from inductance spectroscopic measurements with an EM sensor. The forward problem was solved numerically using the Dodd and Deeds formulation [14]. In the inverse solution, a modified Newton–Raphson method was used to adjust the permeability profile to fit inductances (measured or simulated) in a least-squared sense. In addition, a dynamic rank method was proposed to eliminate the ill-conditioning of the problem in the process of reconstruction. Permeability, conductivity, thickness, and lift-off have been reconstructed from simulated and measured data, which verified this method.

Acknowledgements

The research leading to these results has received funding from the EU Research Fund for Coal and Steel (RFCS) research programme under grant agreement nr. RFSR-CT-2013-00031.

References

1. Peyton, A. J., Davis, C. L., Van Den Berg, F. D., & Smith, B. M. (2014). EM inspection of microstructure during hot processing: the journey from first principles to plant. *Iron & Steel Technology*, *24*(11), 3317-3325.
2. Fukutomi, H., Takagi, T., & Nishikawa, M. (2001). Remote field eddy current technique applied to non-magnetic steam generator tubes. *NDT & E International*, *34*(1), 17-23.
3. Pohl, R., Erhard, A., Montag, H. J., Thomas, H. M., & Wüstenberg, H. (2004). NDT techniques for railroad wheel and gauge corner inspection. *NDT & E International*, *37*(2), 89-94.
4. He, Y., Pan, M., Luo, F., & Tian, G. (2011). Pulsed eddy current imaging and frequency spectrum analysis for hidden defect nondestructive testing and evaluation. *NDT & E International*, *44*(4), 344-352.
5. Lu, M., Peyton, A., & Yin, W. (2017). Acceleration of Frequency Sweeping in Eddy Current Computation. *IEEE Transactions on Magnetics*.
6. Lu, M., Zhao, Q., Hu, P., Yin, W., & Peyton, A. J. (2015, April). Prediction of the asymptotical magnetic polarization tensors for cylindrical samples using the boundary element method. In *Sensors Applications Symposium (SAS), 2015 IEEE* (pp. 1-4). IEEE.
7. Lu, M., Yin, L., Peyton, A. J., & Yin, W. (2016). A novel compensation algorithm for thickness measurement immune to lift-off variations using eddy current method. *IEEE Transactions on Instrumentation and Measurement*, *65*(12), 2773-2779.
8. Ditchburn, R. J., Burke, S. K., & Scala, C. M. (1996). NDT of welds: state of the art. *Ndt & e International*, *29*(2), 111-117.
9. Saguy, H., & Rittel, D. (2007). Flaw detection in metals by the ACPD technique: Theory and experiments. *NDT & E International*, *40*(7), 505-509.
10. Raja, M. K., Mahadevan, S., Rao, B. P. C., Behera, S. P., Jayakumar, T., & Raj, B. (2010). Influence of crack length on crack depth measurement by an alternating current potential drop technique. *Measurement Science and Technology*, *21*(10), 105702.
11. Yin, W., Hao, X. J., Peyton, A. J., Strangwood, M., & Davis, C. L. (2009). Measurement of permeability and ferrite/austenite phase fraction using a multi-frequency electromagnetic sensor. *NDT & E International*, *42*(1), 64-68.
12. Lu, M., Zhu, W., Yin, L., Peyton, A. J., Yin, W., & Qu, Z. (2018). Reducing the Lift-Off Effect on Permeability Measurement for Magnetic Plates From Multifrequency Induction Data. *IEEE Transactions on Instrumentation and Measurement*, *67*(1), 167-174.
13. Avila, J. R. S., How, K. Y., Lu, M., & Yin, W. (2018). A Novel Dual Modality Sensor With Sensitivities to Permittivity, Conductivity, and Permeability. *IEEE Sensors Journal*, *18*(1), 356-362.
14. Dodd, C. V., & Deeds, W. E. (1968). Analytical Solutions to Eddy-Current Probe-Coil Problems. *Journal of applied physics*, *39*(6), 2829-2838.
15. Yin, W., Dickinson, S. J., & Peyton, A. J. (2006). Evaluating the permeability distribution of a layered conductor by inductance spectroscopy. IEEE transactions on magnetics, 42(11), 3645-3651.